Journal of Materials Chemistry C

Accepted Manuscript

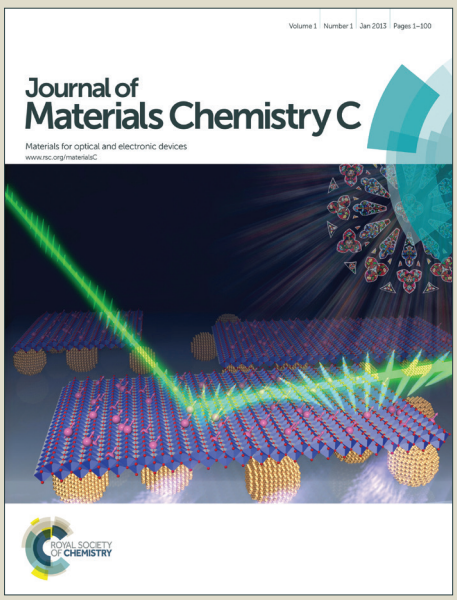

ROYAL SOCIETY OF CHEMISTRY

www.rsc.org/materialsC

Cite this: DOI: 10.1039/c0xx00000x

www.rsc.org/xxxxxx

COMMUNICATION

Third-order nonlinear optical vitreous material derived from mesoporous silica incorporated with Au nanoparticles

Xin Zhang,[a] Wei Luo,[a] Lian-Jun Wang*[a] and Wan Jiang[b]

Received (in XXX, XXX) Xth XXXXXXXXX 20XX, Accepted Xth XXXXXXXXX 20XX

DOI: 10.1039/b000000x

Mesoporous silica SBA-15 encapsulated with Au nanoparticles was consolidated by Spark Plasma Sintering. It is turned out to be an original and facile preparation pathway to incorporate Au nanoparticles in silica glass. Incorporation of Au nanoparticles in silica glass matrix made the obtained glass coloured with dark wine-red due to surface plasmon resonance effect of Au nanoparticles, although the concentration of Au nanoparticles was extreme low (about 0.05wt%). Besides, Z-scan method using femosecond laser pulse was employed to measure the nonlinear optical property of this mesoporous composite derived glass, which exhibited self-focusing feature at 720nm with saturable absorption. The third-order nonlinear refraction index n_2 and absorption coefficient β were 1.74×10^{-18} m^2/W and 5.72×10^{-12} m/W respectively. We believe that this approach could be extended to disperse other metal or semiconductor nanoparticles in glass matrix.

Au nanoparticles (NPs) have received widespread attention due to their fascinating optical, electronic, magnetic and other properties that are different from their bulk counterparts related to quantum confinement effect.[1] An ever growing number of applications in catalysis, sensor, biological labeling and detection, solar cell, optical limiting, optical switching and electronics is explored.[2-8] Among the mentioned applications, nonlinear optical (NLO) area simulates numerous interests of researchers since plasmonic Au NPs possess peculiar optical properties originating from the electromagnetic field induced collective oscillations of surface plasmons (SP).[9] The distinctive feature can cause enhancement of local electric field which improves the third-order NLO susceptibility.[10] However the matrix which is employed to avoid aggregation of Au NPs can influence the photophysical or photochemical process in the specific case of plasmonics.[11] Vitreous matrix composed mainly by silica is a competitive candidate to incorporate Au NPs, as its low dielectric constant is beneficial in improving the nonlinearity of composites.[12] Moreover, silica glass is famous for its extraordinary transparency in the infrared and visible spectral region, excellent thermal and chemical stability and good radiation hardness.[13] Spatially controlling the growth NPs with uniform size and well dispersion in glass matrix cannot be well mastered by traditional glass-making methods, although immense efforts have made to improve the situation. Laser irradiation, ion-exchange and laser direct-writing methods in creating nanostructured particles inside glass merely form hundreds of micrometer surface containing polydispersed NPs.[14] Despite success in preparing Au NPs stabilized in sol-gel derived silica glass,[15] crack may occur when the gel is dried and sintered, in addition, aggregation or coalescence of metal salts or NPs appears during sol-gel polymerization probably.[16,17]

SBA-15 is mesoporous silica with regularly hexagonal pore arrays, changeable pore diameters between 5-30 nm and reactive Si-OH groups on the pore surface,[18] which has been demonstrated to serve as an effective host for filling with various metal and semiconductor nanoparticles.[19] Restricted growth of NPs in the uniform pores of SBA-15 realizes narrow size dispersion of NPs.[20] Herein, we present an effective and versatile route to distribute Au NPs inside silica glass host by taking advantage of SBA-15 with confined Au NPs as starting powders through Spark Plasma Sintering. Because sintering temperature is below the liquidus temperature of composition, it is viewed as a solid-state sintering method.[16] To our knowledge, this is the first report of incorporating relatively uniform Au NPs in silica glass matrix using mesoporous composite based on solid-state sintering.

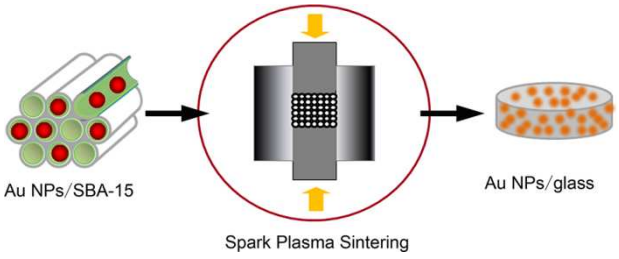

Fig. 1 Diagrammatic representation of the formation procedure of silica glass incorporated with Au NPs

The fabricating procedure for silica glass entrapped with Au NPs (abbreviated as Au NPs/glass) is given in Fig.1. Au NPs were formed inside the channels of SBA-15 through post-synthetic functionalization of the silica surface followed by in situ

reduction of chloroauric acid. Then, synthesized powders were loaded in cylindrical graphite dies with an inner diameter of 12 mm and sintered using spark plasma sintering aperture under a uniaxial pressure of 50 MPa in vacuum at 1293K for 3 min. The whole sintering process just took 10min. The shrink curve of sintering process is referred to Fig.S1 in ESI.

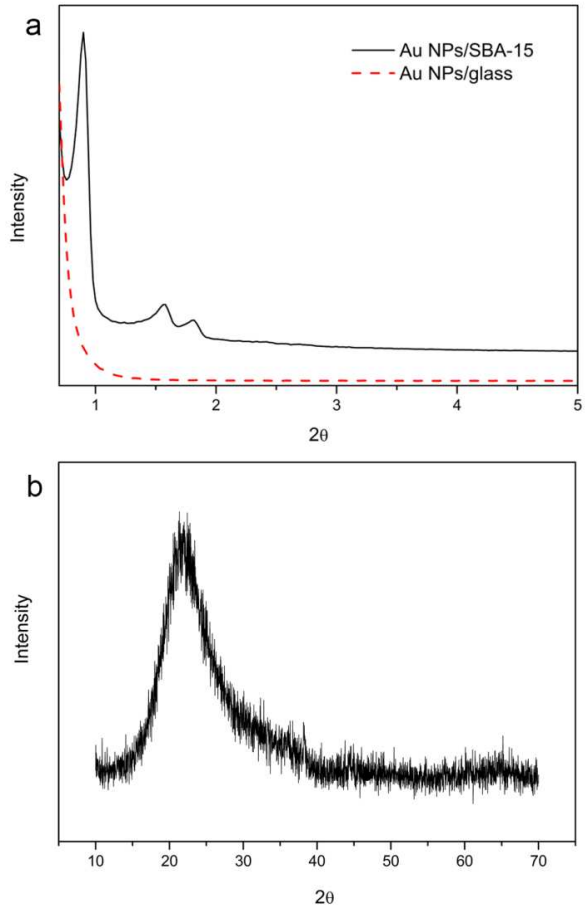

Fig. 2 a) Low-angle XRD patterns of the SBA-15 encapsulated with Au NPs and silica glass containing Au NPs; b) Wide-angle XRD pattern of the as-sintered glass sample containing Au NPs

Before sintering, the encapsulation of Au NPs inside the pore channels of SBA-15 has little impact to the ordered hexagonal mesostructure which is confirmed by low-angle XRD pattern with three indexable peaks seen in Fig.2a. Yet, the obtained bulk sample shows no diffraction peak in this region (Fig.2b), implying that the ordered pore arrays vanish after sintering. The wide-angle XRD pattern of the sintered sample shows a broad diffraction peak located in 21.6° which is signature of amorphous phase. Its location is identical with the (111) feature peak of cristobalite phase which coincides with the hypothesis of glass structure. For Au NPs/SBA-15, a broad diffraction peak emerges in this range either (Fig.S2) which stems from amorphous walls of SBA-15. It thus can be concluded that the sintering process did not cause crystallization of amorphous silica. Normally, the face-centred-cubic structure of crystalline Au is verified by a diffraction peak appearing at 38° which can be indexed as the (111) planes as can be seen in Fig.2S of Au NPs/SBA-15 with high-dose. The indistinct peak of our sintered sample may result from the low concentration of Au NPs in matrix which is beneficial for transparency.

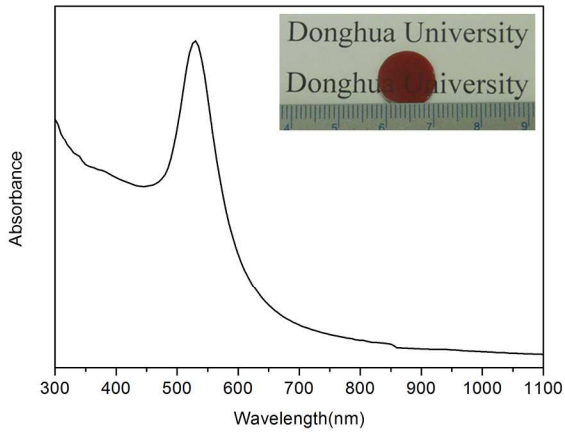

Fig. 3 UV-Vis absorption spectrum of Au NPs/glass sample. The upper inset is the picture of Au NPs/glass sample with wine-red appearance

The mesoporous composite derived glass is optically transparent by visual inspection shown in Fig.3 as the letter beneath can be recognized. Despite the fact that bulk gold appears yellow, the colour of Au NPs/glass has dark wine red appearance depending on SP resonance effect influenced by size and shape of Au NPs as well as the refractive index of the surrounding medium.[9] Fig.3 also shows UV-Vis absorption spectrum of the Au NPs/glass sample. Obviously, an absorption band centres at 528 nm attributed to SP resonance of Au NPs. [21] The UV-Vis absorption spectrum of Au NPs/SBA-15 (Fig.3S) is similar with that of Au NPs/glass where a SP resonance absorption peak can be found. No shift of the SP resonance peak after sintering means the geometry preservation of encapsulated Au NPs. For SiO_2 matrix glass containing noble-metal NPs of Au and Ag, the SP resonance absorption peaks appear near to the edge of the band-to-band transition from the valence d band to the Fermi surface.

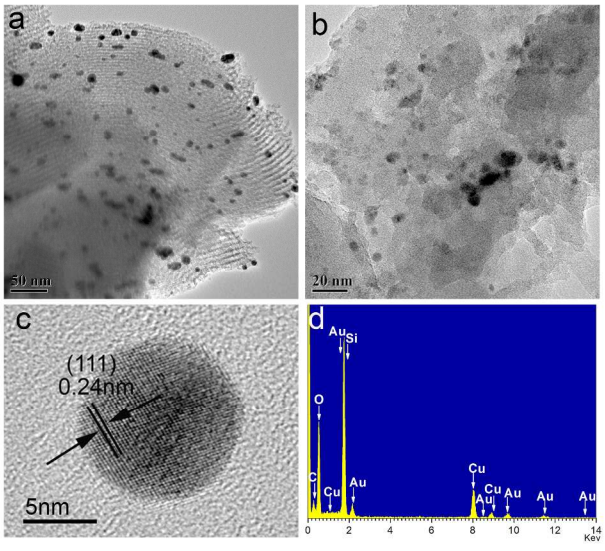

Fig.4 a) TEM image of the SBA-15 encapsulated with Au NPs; b)TEM image of the Au NPs/glass sample; c) HRTEM image of a single Au NP embedded in glass matrix; d) EDX spectrum taken on the dark spherical spots in b), note that the Cu signals come from the copper grid.

TEM image of the Au NPs encapsulated inside the channels of mesoporous SBA-15 is shown in Fig.4a. It is evident that the highly ordered pore channels of SBA-15 is preserved which agrees with the low-angle XRD results (Fig.2a). The detection of Au peaks in energy-dispersive X-ray (EDX) spectrum indicates that dark spherical spots consist of element gold (Fig.S4 in ESI). The regular arrangement of these dark spherical spots reveals that the Au NPs are homogeneously dispersed between the walls of SBA-15. Most of the Au NPs take approximately spherical geometry with diameters in the range of 3-10 nm. As the pore size of SBA-15 is about 6 nm, it is supposed that the growth of Au NPs larger than 6 nm may break the thin pore walls. The same phenomenon has also been reported by Tsung et al in the growth of Au NPs and Ag NPs in mesoporous thin films and nanofibres.[22]

Fig.4b shows a TEM image of the well-dispersed Au NPs in sintered sample, indicating a homogenous distribution feature of NPs in glass matrix as depicted in Fig.1. The diameter of these Au NPs is in the range of 3-10 nm which is consistent with those incorporated in pores of SBA-15. Regarding with the confinement of SBA-15 channels and fast sintering process, the size and morphology of Au NPs are preserved. Our goal to well disperse Au NPs with certain size as optically functional phase in host is achieved. In Fig.4c, an HRTEM image of a single Au nanoparticle is shown, where two distinct sets of lattice fringes are revealed. An interlayer spacing of 0.24 nm is observed which is conform to d spacing of the (111) lattice planes of fcc Au crystal.[23] EDX further confirms that the dark spherical dots within the glass matrix are elemental gold, as shown in Fig.4d.

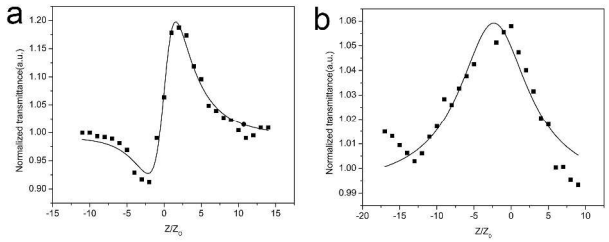

Fig.5 Z-Scan curves of the Au NPs/glass sample recorded at 720 nm. a) and b) are representative CA and OA raw Z-Scans traces (Dots) and theoretical fits (Lines) respectively, where z represents the sample position along z axis and z_0 is the Rayleigh diffraction length of laser beam

The Z-scan measurement is a simple and widely applied technique used to measure both the sign and magnitude of the third-order nonlinear refraction index n_2 and absorption coefficient β via the "open" aperture (OA) and "closed" aperture (CA) methods.[24] It measures the optical nonlinearities through detecting the far-field sample transmittance of a focused Gaussian beam as a function of sample position. Representative CA and OA Z-scan traces for Au NPs/silica glass sample are shown in Fig.5. The signs of the real and imaginary parts of third-order nonlinear optical susceptibility $\chi^{(3)}$ values are easily judged. For CA Z-scan traces (Fig.5a) collected at 720nm, the valley-peak circumstance of the glass transmittance presents a typical self-focusing feature, implying the sign of n_2 which is related to the real part of $\chi^{(3)}$ is positive. Regarding from the enhanced peak transmittance and the suppressed valley in Fig.5a, β associated with the imaginary part of $\chi^{(3)}$ is ought to exhibit saturated absorption with a positive sign. This judgment coincides with the OA Z-scan traces in Fig.5b which is detected as a pronounced peak. Single photon absorption leads to saturated absorption as a bleaching phenomenon of the ground state plasmon band in the case of moderate irradiance.[25] n_2 and β of sintered Au NPs embedded silica glass sample are obtained respectively to be 1.74×10^{-18} m^2/W and 5.72×10^{-12} m/W according to the following equations [26,27]:

$$\Delta T_{p\text{-}v} = 0.406(1-S)^{0.25}\left|\Delta\Phi_0\right| \quad (1)$$

$$\Delta\Phi_0 = kn_2 I_0 L_{eff} \quad (2)$$

$$\Delta T_v = \beta I_0 L_{eff}/2 \quad (3)$$

where $\Delta T_{p\text{-}v}$ is the difference of normalized transmittance between the peak and valley in CA Z-scan results, $\Delta\Phi_0$ is phase modulation, k is the wave number of the light, $L_{eff}=(1-e^{-\alpha L})/\alpha$ is the effective thickness of the sample, α is the linear absorption coefficient and L is the sample thickness which is supposed smaller with respect to the Rayleigh diffraction length $z_0=k\omega^2/2$ of the beam,[27] ΔT_v is the transmittance change in OA Z-scan results. It should underline here that the Au NPs doping concentration is quite low (0.05 wt%) and not all previous reports of Z-scan measurements were performed at such low concentration. Concentration has a crucial influence in calculated values of cubic susceptibility. Generally speaking, within certain concentration range, the higher concentration is adopted, the larger susceptibility values will be got as reported. [28] Optimized dosage concentrations for maximal cubic susceptibility value will be further studied in the future.

As widely known, for NPs entrapped glass, the NLO stems mainly from electronic and thermal contributions which are sensitive to the pulse width. The ultrafast pulse of 200fs used here limits the thermal accumulation, so electronic effect is the main origin of NLO[29] which can provide the fast response time in picosecond or femtosecond scales[30]. The underlying electronic effect for gold NPs at the detected wavelength is through an intraband transition in conduction band between the occupied state near the Fermi level and the unoccupied state.[31] The local near field enhancement associated with SP resonance works efficiently for the NLO enhancement of Au NPs composites in the resonance frequency. It is worth to note that even at off-resonance range, the oscillation of metal NPs plasmon still creates a strengthened electromagnetic field near the surface of the metal NPs that may devotes to the NLO enhancement as the previous literature elaborated[32]. Thus, the NLO properties of Au NPs entrapped glass made from solid-state sintering arise from the intraband transition which is enhanced by local field effect at 720nm.

In conclusion, a novel and facile method to entrap Au NPs inside silica glass matrix at low temperature in a short time is presented through Au NPs/SBA-15 powder transformation. At this processing condition the grain growth of Au NPs is limited,

implying that the consolidation does not influence the size and size distribution of the Au NPs. Moreover, other kinds of nanostructured particles will be easily stabilized in glass matrix once they are confined in the pore channels of SBA-15 following this route. Related reports will be delivered soon. The third-order nonlinear refraction index n_2 and absorption coefficient β of Au NPs embedded silica glass is 1.74×10^{-18} m^2/W and 5.72×10^{-12} m/W at 720nm respectively measuring by Z-scan method.

This work was funded by Natural Science Foundation of China (Nos.51072033, 11179028 and 51272042), "Shu Guang" project supported by Shanghai Municipal Education Commission and Shanghai Education Development Foundation (No.11SG34), Shanghai Rising-Star Program(No.12QH1400100), PCSIRT (No.IRT1221), Key Laboratory of Functional Crystals and Laser Technology (TIPC), CAS, the Fundamental Research Funds for the Central Universities, and DHU Distinguished Young Professor Program.

Notes and references

[a] *State Key Laboratory for Modification of Chemical Fibers and Polymer Materials, College of Material Science & Engineering, Donghua University, Shanghai, 201620, P.R. China. Fax: +86-21-67792855; Tel: +86-21-67792835; E-Mail: wanglj@dhu.edu.cn*

[b] *Engineering Research Center of Advanced Glasses Manufacturing Technology, MOE, Donghua University, Shanghai, 201620, P.R. China*

† Electronic Supplementary Information (ESI) available: The details of Au NPs/SBA-15 powder synthesis and its EDX characerization.The shrink curve of the composite powder sintering. See DOI: 10.1039/b000000x/

1 Y. Sun and Y. Xia, *Science*,2002,**298**,2176-2180.

2 A. Wittstock, V. Zielasek, J. Biener, C. M. Friend and M. Bäumer, *Science*,2010,**327**,319-323;

3 J. N. Anker, W. P. Hall, O. Lyandres, N. C. Shah, J. Zhao, R. P. Van Duyne, *Nat. Mater.*,2008,**7**,442-453; N. M. Figueiredo, T. Kubart, J. A. Sanchez-Garcia, R. Escobar Galindo, A. Climent-Font and A. Cavaleiro, *J. Appl. Phys.*,2014,**115**, 063512-1-14.

4 T. K. Sau, A. L. Rogach, F. Jäckel, T. A. Klar and J. Feldmann, *Adv. Mater.*,2010,**22**,1805-1825.

5 X. Xu, J. Cui, J. Han, J. Zhang, Y. Zhang, L. Luan, G. Alemu, Z. Wang, Y. Shen, D. Xiong, W. Chen, Z. Wei, S. Yang, B. Hu, Y. Cheng and M. Wang, *Scientific Reports*,2014,**4**,3961-1-8.

6 R. Philip, P. Chantharasupawong, H. Qian, R. Jin and J. Thomas, *Nano Lett.*,2012,**12**,4661-4667.

7 J. Qiu, X. Jiang, C. Zhu, M. Shirai, J. Si, N. Jiang and K. Hirao, *Angew. Chem. Int. Ed.*,2004,**43**,2230-2234.

8 T. Jain, Q. Tang, T. Bjørnholm and K. Nørgaard, *Acc. Chem. Res.*,2014,**47**,2-11.

9 M. C. Daniel and D. Astruc, *Chem. Rev.*, 2004,**104**,293-346.

10 E. Xenogiannopoulou, K. Iliopoulos, S. Couris, Karakouz, T. A. Vaskevich and I. Rubinstein, *Adv. Funct. Mater.*, 2008,**18**,1281-1289.

11 V. N. Sigaev, V. I. Savinkov, S. V. Lotarev, G. Y. Shakhgildyan, R. Lorenzi and A. Paleari, *Nanotechnology*,2013,**24**,225302.

12 X. Zheng, M. Feng, Z. Li, Y. Song and H. Zhan, *J. Mater. Chem. C*, 2014, DOI: 10.1039/C3TC32410A.

13 K. Kajihara, M. Hirano and H. Hosono, *Chem. Comm.*,2009,**18**, 2580-2582.

14 F. Goutaland, J. P. Colombier, M. C. Sow, N. Ollier and F. Vocanson, *Opt Express*,2013,21,31789-31799; A. Simo, J. Polte, N. Pfänder, U. Vainio, F. Emmerling, K. Rademann, *J. Am. Chem. Soc.*,2012,**134**,18824-33; S. J. Henley,M. J. Beliatis, V. Stolojan and S. R. P. Silva, *Nanoscale*,2013,**5**,1054-1059.

15 S. T. Selvan, T. Hayakawa, M. Nogami,Y. Kobayashi, L. M. Liz-Marzán, Y. Hamanaka and A. Nakamura, *J. Phys. Chem. B*,2002,**106**,10157-10162.

16 M. Toki, T. Takeuchi, S. Miyasita and S. Kanbe, *J. Mater. Sci.*,1992,**27**,2857-2862.

17 S. Bharathi and O. Lev, *Chem. Commun.*,1997,**24**,2303-2304.

18 D. Zhao, J. Feng, Q. Huo, N. Melosh, G. H. Fredrickson, B. F. Chmelka and G. D. Stucky, *Science,*1998, **279**, 548-552; M. H. Huang, A. C. and P. Yang, *Chem. Commun.*,2000,1063-1064; L. Tian, Q. Yang, Z. Jiang,Y. Zhu,Y. Pei, M. Qiao and K. Fan, *Chem. Commun.*,2011,**47**, 6168-6170.

19 Z. Kónya, V. F. Puntes, I. Kiricsi, J. Zhu, A. P. Alivisatos and G. A. Somorjai, *Nano Lett.*,2002,**2**,907-910; C. Yang, P. Liu, Y. Ho, C. Chiu and K. Chao, *Chem. Mater.*,2003,**15**,275-280.

20 T. Asefa and R. B. Lennox, *Chem. Mater.*,2005,**17**,2481-2483; Y. Zhu, D. Wang, L. Zhang, F. Sun, J. Xu, S. Jiang and Q. Yu, *RSC Adv.*,2013,**3**,10154-10157; J. Yang, K. Hidajat, S. Kawi, *J. Mater. Chem.*,2009,**19**,292-298.

21 N. J. Halas, S, Lal, W, Chang, S. Link and P. Nordlander, *Chem. Rev.*, 2011,**111**,3913-3963.

22 C. K. Tsung, W. Hong, Q. Shi, X. Kou, M. H. Yeung, J. Wang and G. D. Stucky, *Adv. Funct. Mater.*, 2006,**16**, 2225-2230.

23 J. Zeng, J. Huang, C. Liu, C. Wu, Y. Lin, X. Wang, S. Zhang, J. Hou and Y. Xia, *Adv. Mater.*, 2010,**22**, 1936-1940.

24 G. Nootz, L. A. Padilha, P. D. Olszak, S. Webster, D. J. Hagan, E. W. V. Stryland, L. Levina, V. Sukhovatkin, L. Brzozowski and E. H. Sargent, *Nano. Lett.*, 2010, **10**, 3577-3582.

25 Y. H. Lee, Y. Yan, L. Polavarapu and Q. H. Xu, *Appl. Phys. Lett.*, 2009,**95**,023105.

26 Y. Chen, Q. Nie, T. Xu, S. Dai, X. Wang and X. Shen, *J. Non-Cryst. Solids*,2008,**354**,3468-3472.

27 M. Sheik-Bahae, A. A. Said, T. Wei, D. J. Hagan and E. W. V. Stryland, *IEEE J. Quantum Electron.*, 1990, **26**, 760-769.

28 H. I. Elim, W. Ji, A. H. Yuwono, J. M. Xue and J. Wang, *Appl. Phys. Lett.*, 2003,**82**, 2691-2693.

29 Q. Q. Wang , J. B. Han, H. M. Gong, D. J. Chen, X. J. Zhao, J. Y. Feng and J. J. Ren, *Adv. Funct. Mater.*, 2006,**16**,2405-2408.

30 Y. Hamanaka, N. Okada, K. Fukagawa, A. Nakamura, Y. Tai and J. J. Murakami, *Phys.Chem. C*, 2012,**116**, 10760-10765.

31 J. L. Gu, J. L. Shi, G. J. You, L. M. Xiong, S. X. Qian, Z. L. Hua and H. R. Chen, *Adv. Mater.*, 2005,**17**,557-560.

32 M. Saboktakin, X. Ye, S. Ju Oh, S. H. Hong, A. T. Fafarman, U. K. Chettiar, N. Engheta, C. B. Murray and C. R. Kagan, *ASC Nano*, 2012,**6**, 8758-8766.

Table of Contents

Color graphic:

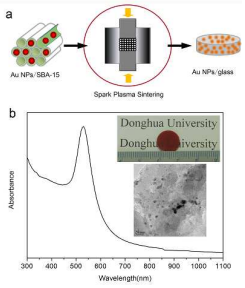

Text:

A novel method is introduced to prepare gold nanoparticles embedded silica glass matrix with third-order nonlinear optical property.